



Article

A Novel Method for Digital Reconstruction of the Mucogingival Borderline in Optical Scans of Dental Plaster Casts

Leonard Simon Brandenburg ^{1,*}, Stefan Schlager ¹, Lara Sophie Harzig ¹, David Steybe ¹, René Marcel Rothweiler ¹, Felix Burkhardt ², Benedikt Christopher Spies ², Joachim Georgii ³ and Marc Christian Metzger ¹

- ¹ Medical Center—University of Freiburg, Center for Dental Medicine, Department of Oral and Maxillofacial Surgery, Faculty of Medicine, University of Freiburg, Hugstetter Str. 55, 79106 Freiburg, Germany; stefan.schlager@anthropologie.uni-freiburg.de (S.S.); lara.sophie.harzig@uniklinik-freiburg.de (L.S.H.); david.steybe@uniklinik-freiburg.de (D.S.); rene.rothweiler@uniklinik-freiburg.de (R.M.R.); marc.metzger@uniklinik-freiburg.de (M.C.M.)
- ² Medical Center—University of Freiburg, Center for Dental Medicine, Department of Prosthetic Dentistry, Faculty of Medicine, University of Freiburg, Hugstetter Str. 55, 79106 Freiburg, Germany; felix.burkhardt@uniklinik-freiburg.de (F.B.); benedikt.spies@uniklinik-freiburg.de (B.C.S.)
- ³ Fraunhofer Institute for Digital Medicine MEVIS, Bremen, Max-von-Laue-Str. 2, 28359 Bremen, Germany; joachim.georgii@mevis.fraunhofer.de
- * Correspondence: leonard.brandenburg@uniklinik-freiburg.de; Tel.: +49-761-270-49240



Citation: Brandenburg, L.S.; Schlager, S.; Harzig, L.S.; Steybe, D.; Rothweiler, R.M.; Burkhardt, F.; Spies, B.C.; Georgii, J.; Metzger, M.C. A Novel Method for Digital Reconstruction of the Mucogingival Borderline in Optical Scans of Dental Plaster Casts. *J. Clin. Med.* **2022**, *11*, 2383. <https://doi.org/10.3390/jcm11092383>

Academic Editors: Joseph Nissan and Gavriel Chaushu

Received: 9 April 2022

Accepted: 22 April 2022

Published: 24 April 2022

Publisher's Note: MDPI stays neutral with regard to jurisdictional claims in published maps and institutional affiliations.



Copyright: © 2022 by the authors. Licensee MDPI, Basel, Switzerland. This article is an open access article distributed under the terms and conditions of the Creative Commons Attribution (CC BY) license (<https://creativecommons.org/licenses/by/4.0/>).

Abstract: Adequate soft-tissue dimensions have been shown to be crucial for the long-term success of dental implants. To date, there is evidence that placement of dental implants should only be conducted in an area covered with attached gingiva. Modern implant planning software does not visualize soft-tissue dimensions. This study aims to calculate the course of the mucogingival borderline (MG-BL) using statistical shape models (SSM). Visualization of the MG-BL allows the practitioner to consider the soft tissue supply during implant planning. To deploy an SSM of the MG-BL, healthy individuals were examined and the intra-oral anatomy was captured using an intra-oral scanner (IOS). The empirical anatomical data was superimposed and analyzed by principal component analysis. Using a Leave-One-Out Cross Validation (LOOCV), the prediction of the SSM was compared with the original anatomy extracted from IOS. The median error for MG-BL reconstruction was 1.06 mm (0.49–2.15 mm) and 0.81 mm (0.38–1.54 mm) for the maxilla and mandible, respectively. While this method forgoes any technical work or additional patient examination, it represents an effective and digital method for the depiction of soft-tissue dimensions. To achieve clinical applicability, a higher number of datasets has to be implemented in the SSM.

Keywords: statistical shape model; mucogingival borderline; implant planning; soft tissue dimensions; virtual planning

1. Introduction

Osseo-integrated implants have emerged as the gold standard in dental care since their invention by Brånemark in the 1970s [1,2]. Highly aesthetic results, comfort in wear and the preservation of neighboring teeth describe only a few of the advantages that come with the use of implant-supported prostheses [3,4]. Unlike early implant systems, today's modern implants achieve long-term survival rates and may last for decades, making them a reliable restorative option [5,6]. Moreover, sophisticated screening tools [7,8] help to identify patients suitable for implant treatment [9,10]. In addition to the continuous improvement of implant designs, pre-operative planning options have developed decisively to improve long-term stability of implants. Modern computer-tomography imaging [11] and the invention of computer-assisted surgery [12] allow advanced implant site assessment and pre-operative virtual planning [13–18]. Especially complex implant cases, e.g.,

patients with syndromal malformations [19–21], reduced mouth opening [22] or poor bone quality [23], require an impeccable preoperative planning to enable safe and successful implant placement. Modern planning software allows the determination of an ideal implant position that matches both the patient-specific anatomy and the requirements of the desired dental prosthesis [13–18]. Furthermore, pre-operative virtual planning increases the efficiency of the whole treatment procedure [24,25].

Current literature reports that pre-operative planning should consider soft-tissue dimensions to guarantee long-term success [26–29]. In fact, recent studies have shown that an adequate amount of attached gingiva around dental implants leads to increased hard- and soft-tissue stability [30,31], better esthetic results [32], reduced plaque accumulation and a lower incidence of peri-implant mucositis [33]. It can be stated that implants should only be placed in regions of the jaw covered with a sufficient amount of attached gingiva.

In healthy patients, the attached gingiva extends from the level of the marginal gingiva to the mucogingival borderline (MG-BL). The marginal gingiva is easily identifiable at the borderline between mucosa and tooth (referred to as mucous–tooth borderline, “MT-BL” in the following). The MG-BL describes the transition from attached to flexible mucosa [34]. This junction line becomes obscured by contact pressure on the gingiva during conventional impression taking. In contrast, intra-oral scans (IOS) can depict the MG-BL due to the difference in color appearance of attached gingiva and free mucosa. However, despite increasing digitalization in dentistry, in some cases the use of plaster casts is preferred, due to the haptic features of physical models or the lack of modern intra-oral scanners [35,36]. Recent review articles on dental implant planning still describe the use of plaster casts as the current state of the art [17]. It should be noted that scans of plaster models do not allow to identify the MG-BL when fed into the virtual planning process via digitization [16,17]. Considering the fundamental relevance of the attached gingiva for long-term success of dental implants, different approaches were proposed to reconstruct the MG-BL in plaster casts [37–39]. The aim of this study was to visualize the course of the MG-BL based on the information available from conventionally fabricated plaster casts using a statistical shape model (SSM), which processes empirical anatomical data. Moreover, the aim of this study was to assess if and to what degree the shape of MG-BL can be statistically modeled as a function of MT-BL. The working hypothesis can be stated as follows: it is possible to derive the morphology of the MG-BL of healthy individuals from geometric information provided by a digitized plaster cast using a digital workflow.

2. Materials and Methods

This study was approved by the ethics committee of the Albert-Ludwigs-University Freiburg, Germany (No. 251/20, renewed by No. 21/1451) and was registered in the German Clinical Trials Register (No. DRKS00027435). All participants gave written informed consent for study implementation.

Data processing, analyses and shape model creation were performed using the R-packages Morpho, Rvcg [40,41] and RvtkStatismo [42], which are available for the statistical/mathematical platform R [43].

2.1. Study Design

In this prospective study, conventional dental impressions, as well as IOS, were taken from dental students and employees of the Faculty of Dentistry of the University of Freiburg (see Sections 2.3 and 2.4). Based on the acquired IOS, an SSM was generated, which captured the shape variability of the MG-BL and the MT-BL within the study sample. The plaster casts were scanned and saved as digital models. For each digitized model, the MG-BL was reconstructed using a temporarily created SSM in a Leave-One-Out Cross Validation (LOOCV) (see Sections 2.5 and 2.6). Differences between the calculated and the original MG-BL were determined by comparison of the IOS with the SSM-based reconstruction to assess the accuracy of this workflow (see Section 2.7).

2.2. Inclusion and Exclusion Criteria

Dental medicine students and employees aged over 18 years at the Faculty of Dentistry of the University of Freiburg, who signed an informed consent, were considered for study implementation. The following inclusion criteria were defined for this study: adequate oral hygiene, no periodontal or gingival diseases and no existent dental implants. All participants had a continuous dental arch with existent teeth 17–27 and 37–47 (FDI-scheme).

Subjects under 18 years of age or with any type of periodontal or gingival disease, dental implants or missing teeth (except wisdom teeth) were excluded from the study.

2.3. Creation of IOS and Plaster Casts

The IOS were performed using an intra-oral scanner (Trios 4, 3Shape, Copenhagen, Denmark). The scanning procedure was performed according to the manufacturer's instructions, and the suggested scan paths were applied. Extent areas of the IOS were cropped if necessary and the mesh was exported as Polygon File (PLY), which includes color information. Plaster casts were produced using alginate impression material (Alginoplast®, Kulzer Mitsui Chemicals Group, Hanau, Germany) and dental stone (pico-crema soft® type 3 DIN EN ISO 6873, Picodent, Wipperfürth, Germany). Digitization was performed using an optical scanner (E3, 3Shape), and the data was equally exported as PLY files (see Figure 1).

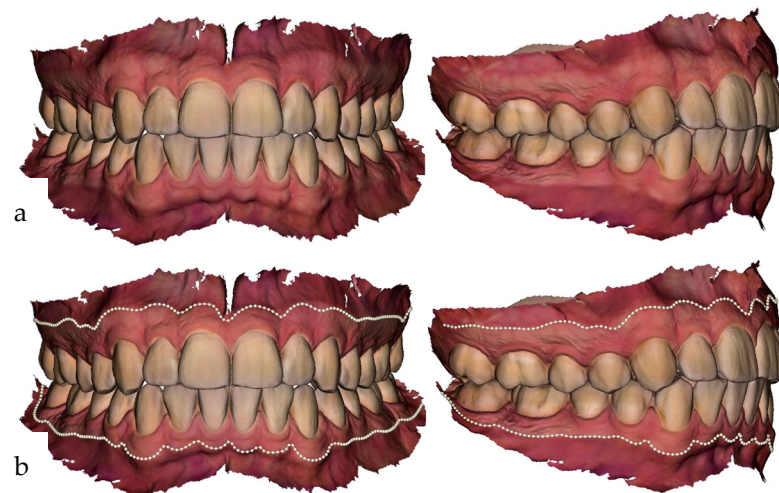


Figure 1. The MG-BL can be identified by the difference in color of attached gingiva and free mucosa. The MT-BL is clearly visible at the junction between tooth and gingiva (a). The MT-BL and MG-BL are placed in 3D Slicer using curves based on sliding semi-landmarks (b).

2.4. Preparation of the Data

Two different curves, which indicate the course of the MT-BL and the MG-BL, were set on the IOS using the open-source software 3D Slicer [44] (see Figures 1b and 2). The curves were set using sliding semi-landmarks [45] (see Figure 2). The MT-BL was set at the transition from mucous membrane to tooth using 560 semi-landmarks. The tip of the interdental papillae was marked additionally with one landmark from both buccal and oral side to capture the morphology of the MT-BL in detail. The MG-BL was set along the transition from attached to flexible mucosa using 150 semi-landmarks (see Figure 2). To minimize noise along the curves, landmarks were allowed to slide along the curves [45]. Furthermore, four identical anatomical landmarks were set on each of the surface scans and the corresponding digitized models for superimposition of the two surfaces later on.

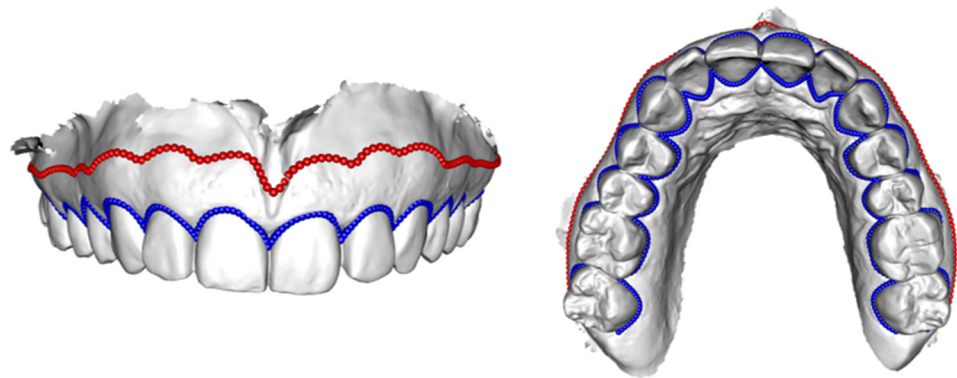


Figure 2. Detailed depiction of the sliding semi-landmarks set along the MT-BL (blue) and MG-BL (red). To achieve a proper representation of the MT-BL the tip of each interdental papilla was annotated with one additional landmark from each side (oral and buccal).

2.5. Statistical Shape Model

Statistical shape modeling is a validated method for automatic processing of medical imaging data [46]. SSM are computed from a set of spatially registered individual shapes—e.g., anatomical structures—from which they “learn” the variability of valid shapes. SSM model that variability and parametrize the boundaries within which the shape is allowed to vary as a probability distribution [47]. Thus, in addition to the mere identification of anatomical structures, the shape of missing or damaged structures can be computed within medical imaging datasets using SSM [48–52]. The clinical use of SSM for creating digital dental wax-ups was demonstrated recently [53]. To extend the applicability of shape modeling in the field of implant planning, an SSM to predict the MG-BL based on the morphology of the MT-BL was generated. A separate SSM for the upper and lower jaw was deployed based on the combined landmark information annotated in the training data (see Figure 1). To build the SSM, the semi-landmarks were allowed to slide along the curves, minimizing Thin Plate Spline-bending energy, in order to remove noise associated with inconsistent digitization [45]. To remove differences regarding rotation and spatial position, a Procrustes registration was applied based on the MT-BL coordinates. The registration was restricted to the MT-BL as a known structure. Following the registration, a shape model was computed using Principal Component Analysis [54–56].

2.6. Reconstruction of the MG-BL

The SSM was used to estimate the missing MG-BL on digitized plaster casts. To avoid statistical self-inference, a LOOCV scheme was applied: for each patient, an SSM was computed from the remaining data (excluding the investigated case) and was used to predict the patient’s mucogingival line. The prediction was performed by computing the posterior mean based on the available MT-BL [56].

2.7. Accuracy Analysis

The distance between each point in the actual MG-BL (as detected in the IOS) and the closest counterpart on the predicted MG-BL (as calculated by the SSM) was determined to estimate the prediction error. As the error distribution was non-gaussian, reporting the error as mean and accompanying standard deviation was not applicable. To obtain an idea about the distribution of the error, the median, as well as the 10th and 90th percentile from the pooled error values, were computed. 10th and 90th percentile were given in brackets following the median value.

3. Results

Eighty-two participants volunteered for study implementation. A total of 74 individuals were included in the study. Eight patients were excluded due to missing teeth. Of

the 74 included individuals, 73 IOS of the maxilla and 71 IOS of the mandible were used for further examination. The analyzed IOS included the surrounding mucous membrane including colored texture information. Four scans were not analyzed because they were afflicted by mirroring artifacts. The age of the study participants was between 22 and 55 years with a mean age of 25.5 ± 4.4 years. Digital evaluation and accuracy analysis could be conducted successfully with the mentioned methods (see Figure 3).

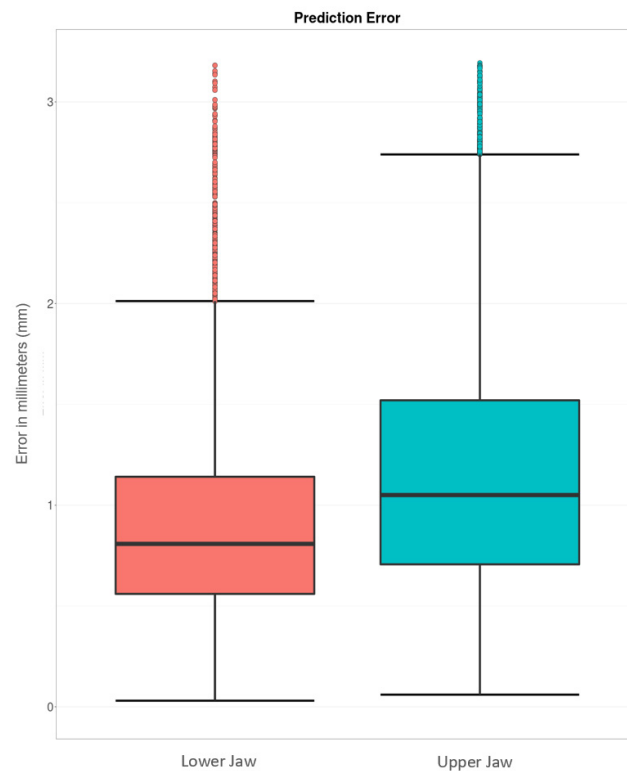


Figure 3. Boxplot showing the error distribution of the reconstruction of the MG-BL on all tested individuals using the developed SSM.

3.1. Maxilla

The median error for MG-BL reconstruction of the maxilla was 1.06 mm (0.49 mm–2.15 mm) (see boxplot in Figure 3). Figure 4 depicts the best (left side) and worst (right side) prediction of MG-BL.

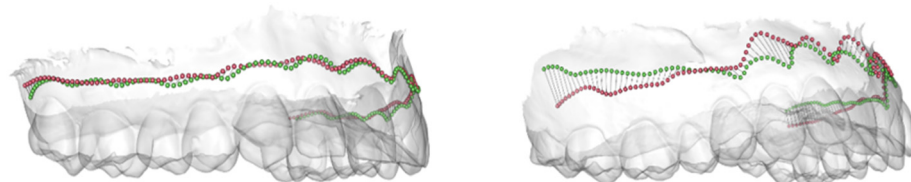


Figure 4. Best (left) and worst (right) prediction of the MG-BL of the maxilla based on the average error.

3.2. Mandible

The median error for MG-BL reconstruction of the mandible was 0.81 mm (0.38 mm–1.54 mm) (see boxplot in Figure 3). Figure 5 depicts the best (left side) and worst (right side) prediction of MG-BL.

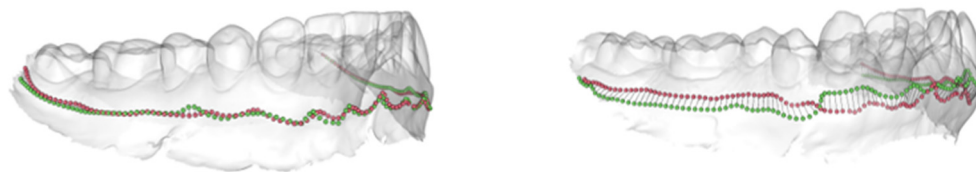


Figure 5. Best (left) and worst (right) prediction of the MG-BL of the mandible based on the average error.

4. Discussion

In this study, reconstruction of the MG-BL on digitized plaster casts was successfully performed using an SSM. With a median reconstruction accuracy of 0.81 mm for the lower jaw and 1.06 mm for the upper jaw, this workflow can be considered as an accurate reconstruction method. The generated SSM contains the shape information of two anatomical structures of 74 healthy individuals: the MT-BL and the MG-BL, which were extracted from IOS. Therefore, the reconstruction implies a strong covariation between the shape of the MT-BL and the MG-BL to successfully perform a reconstruction. Regarding the achieved accuracy of the proposed workflow, this assumption could be confirmed within the selected study group, even if the generation of the SSM was performed regardless of age or sex. As the evaluation was performed using an LOOCV, self-interference of the SSM with the investigated individual was avoided. This means that the digital scan of each plaster cast was presented to a temporary version of the deployed SSM like an unknown individual. Hence, the presented workflow manages to calculate the best possible representation of the MG-BL using an anatomical SSM, without requiring any information of the patient's anatomy. This can be advantageous if only plaster casts are available, and the patient cannot attend further examination. Compared to other methods for depiction of the MG-BL [37,38] the presented workflow is fully digital and forgoes patient consultation and time-consuming and costly technical work. As digital platforms and artificial intelligence networks are increasingly used to obtain health-related information by both dental health-care professionals [57,58] and patients [59], this method addressed the upcoming trend of computerized health-care.

Historically, pre-operative planning of dental surgery was performed using physical models solely. Hereby all information required had to be depicted within or on top of the physical plaster cast to be used for planning purposes. Chee et al. presented an elaborate technique to fabricate master casts, which simulate the soft tissue dimensions using polyether impression material [60]. As this work was presented at a time when digital planning had not yet entered clinical routine, it was not designed to be fed into digital workflows. The manual steps required by this technique are a perfect example for the elaborate procedures that were necessary in the absence of computerized planning methods. Tarnow et al. [37] and Kaku et al. [38] presented methods for transferring MG-BL into virtual datasets, about twenty years later, when digital implant planning was already established. Both workflows involve marking the attached gingiva in the patient's mouth: Tarnow et al. transfer the MG-BL to a plaster cast using an indelible pencil mark and subsequently fabricate a radiographic stent, which indicates the course of the MG-BL [37]. Kaku et al. mark the attached gingiva with radio-opaque sealer, which is then exposed during a cone-beam computed tomography (CBCT) scan [38]. While both authors report successful transfer of the MG-BL into virtual datasets, no accuracy analysis was presented. Both techniques come along with a time-consuming patient examination and a remarkable amount of technical work to be done before the MG-BL can be depicted digitally. Our workflow only requires the digital annotation of the MT-BL to calculate the missing information about the MG-BL and does not require a dental technician. Future research efforts can facilitate the procedure even further by automatizing the setting of landmarks using algorithmic support.

However, it must be noted that the presented workflow comes with several limitations. First of all, the SSM only calculates an estimation of the MG-BL, which may never be fully

identical to the actual MG-BL of the patient. Even if the reported accuracy of this workflow suggests acceptable results within the selected study group, peculiarities of patient-specific anatomy, dental health and a multitude of other factors must be considered regarding their impact on the shape of the MG-BL. Recent publications presented a correlation between age and sex with gingival biotype [61,62]. Possible interference of patient specific features with the MG-BL are therefore likely, but not considered in the current version of the SSM yet. Moreover, the current version of the SSM does not include data about edentulous or partially edentulous patients. As tooth loss affects alterations in soft tissue dimensions [63], the data of (partially) edentulous jaws should be captured in an advanced version of the SSM to create a useful tool for implant planning. To enhance the SSM, patient specific features such as age, sex or ethnicity should be considered to take their possible effects on soft tissue dimensions into account. In this context, it must be noted that data curation may be possible in high numbers among healthy individuals, but those patients who may benefit the most from soft tissue reconstruction prior to implant planning are rare. This may lead to underrepresentation of the according anatomical shapes within the SSM and poor results for patients with unusual oral anatomy, such as clefts or syndromal malformations. The large amount of data required and the difficulties in estimating the learning success of artificial intelligence are a frequently mentioned barrier to the development of algorithm-based applications in medicine [64–66]. In this feasibility study, the reconstruction of the MG-BL was performed within a study group consisting of healthy individuals only.

To date, there is no study that describes the calculation of missing periodontal soft-tissue information in a digital dataset. Unlike available methods, the SSM can augment incomplete information by using empirical anatomical data without additional patient consultation. In clinical scenarios, this may be especially useful when plaster casts are scanned for planning purposes or IOS were performed insufficiently in the area of the MG-BL. As SSM-based reconstruction methods were recently reported as a viable way for computing digital wax-ups in a digital implant planning workflow [53], this study presents a relevant extension concerning relevant soft-tissue dimensions. In combination, the SSM could calculate important prosthodontic (e.g., dental wax-up of missing teeth) and periodontal information (e.g., supply of attached gingiva), which is necessary for proper implant planning. To gain clinical applicability, the inclusion of a high number of training data sets, which depict a multitude of different intra-oral situations, would be necessary. Although further work is required to extend the applicability of the SSM on (partially) edentulous patients, the rapid and feasible functionality of SSM makes it an effective digital method, which may save time and costs in future implant planning applications.

5. Conclusions

As the attached gingiva has a crucial role for the long-term success of dental implants, it should be considered in dental implant planning. Plaster casts are frequently used for implant planning but do not depict the MG-BL properly. Thus, the supply of attached gingiva on the alveolar ridge cannot be determined based on this data. In this study, a novel method for the depiction of the MG-BL in implant planning datasets was described. In contrast to methods described previously, no additional patient examination or elaborate technical work is necessary for this purpose. By implementing various anatomical datasets in an SSM, a digital reconstruction of the MG-BL can be performed by simply placing digital landmarks along the MT-BL. Using this method, the course of the MG-BL can be calculated in a fast and viable way during a planning session displaying the amount of attached gingiva. As the empirical knowledge of the current version of the SSM does not consider the multitude of different anatomical shapes among dental implant patients yet, further implementation of datasets is necessary to obtain clinical applicability of the presented workflow.

Author Contributions: Conceptualization, L.S.B.; methodology, S.S.; validation, M.C.M., F.B. and B.C.S.; formal analysis, S.S.; investigation, S.S.; data curation, L.S.H.; writing—original draft preparation, L.S.B.; writing—review and editing, L.S.H., S.S., M.C.M., R.M.R., D.S. and J.G.; supervision, M.C.M. All authors have read and agreed to the published version of the manuscript.

Funding: The article processing charge was funded by the Baden-Wuerttemberg Ministry of Science, Research and Art and the University of Freiburg in the funding program Open Access Publishing.

Institutional Review Board Statement: The study was conducted in accordance with the Declaration of Helsinki and approved by the Institutional Review Board (or Ethics Committee) of Albert-Ludwigs-University Freiburg, Freiburg Germany (Protocol No. 251/20 and 21/1451).

Informed Consent Statement: Informed consent was obtained from all subjects involved in the study.

Data Availability Statement: The data presented in this study are available on request from the corresponding author. The data are not publicly available due to ethical restrictions.

Acknowledgments: This work was conducted as part of the doctoral degree in dentistry (Dr. med. dent.) of L.S.H. at the Medical Faculty of the University of Freiburg.

Conflicts of Interest: The authors declare no conflict of interest.

Abbreviations

| | |
|-------|------------------------------------|
| CBCT | cone-beam computed tomography |
| FDI | Fédération Dentaire Internationale |
| IOS | Intraoral scanner |
| LOOCV | Leaving-One-Out Cross Validation |
| MG-BL | mucogingival borderline |
| MT-BL | mucous-tooth borderline |
| PLY | Polygon File |
| SSM | Statistical Shape Model |

References

1. Brånemark, P.I.; Hansson, B.O.; Adell, R.; Breine, U.; Lindström, J.; Hallén, O.; Ohman, A. Osseointegrated implants in the treatment of the edentulous jaw. Experience from a 10-year period. *Scand. J. Plast. Reconstr. Surg. Suppl.* **1977**, *16*, 10007349596.
2. Brånemark, P.-I.; Zarb, G.A.; Albrektsson, T. *Tissue-Integrated Prosthesis: Osseointegration in Clinical Dentistry*; Quintessence: Chicago, IL, USA, 1985; ISBN 978-0-86715-129-9.
3. Belser, U.C.; Buser, D.; Hess, D.; Schmid, B.; Bernard, J.P.; Lang, N.P. Aesthetic implant restorations in partially edentulous patients—a critical appraisal. *Periodontology 2000* **1998**, *17*, 132–150. [[CrossRef](#)]
4. Saadoun, A.P.; LeGall, M.; Touati, B. Selection and ideal tridimensional implant position for soft tissue aesthetics. *Pract. Periodontics Aesthetic Dent. PPAD* **1999**, *11*, 1063–1072. [[PubMed](#)]
5. Block, M.S. Dental Implants: The Last 100 Years. *J. Oral Maxillofac. Surg. Off. J. Am. Assoc. Oral Maxillofac. Surg.* **2018**, *76*, 11–26. [[CrossRef](#)] [[PubMed](#)]
6. Levin, L.; Halperin-Sternfeld, M. Tooth preservation or implant placement: A systematic review of long-term tooth and implant survival rates. *J. Am. Dent. Assoc.* **1939** **2013**, *144*, 1119–1133. [[CrossRef](#)] [[PubMed](#)]
7. Häggman-Henrikson, B.; Ekberg, E.; Ettlin, D.A.; Michelotti, A.; Durham, J.; Goulet, J.-P.; Visscher, C.M.; Raphael, K.G. Mind the Gap: A Systematic Review of Implementation of Screening for Psychological Comorbidity in Dental and Dental Hygiene Education. *J. Dent. Educ.* **2018**, *82*, 1065–1076. [[CrossRef](#)] [[PubMed](#)]
8. Contaldo, M.; Della Vella, F.; Raimondo, E.; Minervini, G.; Buljubasic, M.; Ogodescu, A.; Sinescu, C.; Serpico, R. Early Childhood Oral Health Impact Scale (ECOHIS): Literature review and Italian validation. *Int. J. Dent. Hyg.* **2020**, *18*, 396–402. [[CrossRef](#)] [[PubMed](#)]
9. Herrmann, I.; Lekholm, U.; Holm, S.; Kultje, C. Evaluation of patient and implant characteristics as potential prognostic factors for oral implant failures. *Int. J. Oral Maxillofac. Implant.* **2005**, *20*, 220–230.
10. Paquette, D.W.; Brodala, N.; Williams, R.C. Risk Factors for Endosseous Dental Implant Failure. *Dent. Clin.* **2006**, *50*, 361–374. [[CrossRef](#)] [[PubMed](#)]
11. Ruprecht, A. Oral and Maxillofacial Radiology: Then and Now. *J. Am. Dent. Assoc.* **2008**, *139*, S5–S6. [[CrossRef](#)] [[PubMed](#)]
12. Ranev, D.; Teixeira, J. History of Computer-Assisted Surgery. *Surg. Clin. N. Am.* **2020**, *100*, 209–218. [[CrossRef](#)] [[PubMed](#)]
13. Jansen, J.; Schreurs, R.; Dubois, L.; Maal, T.J.J.; Gooris, P.J.J.; Becking, A.G. The advantages of advanced computer-assisted diagnostics and three-dimensional preoperative planning on implant position in orbital reconstruction. *J. Cranio-Maxillofac. Surg.* **2018**, *46*, 715–721. [[CrossRef](#)] [[PubMed](#)]

14. Scherer, M.D. Presurgical Implant-Site Assessment and Restoratively Driven Digital Planning. *Dent. Clin. N. Am.* **2014**, *58*, 561–595. [[CrossRef](#)] [[PubMed](#)]
15. Kernen, F.; Kramer, J.; Wanner, L.; Wismeijer, D.; Nelson, K.; Flügge, T. A review of virtual planning software for guided implant surgery—Data import and visualization, drill guide design and manufacturing. *BMC Oral Health* **2020**, *20*, 251. [[CrossRef](#)]
16. D’haese, J.; Ackhurst, J.; Wismeijer, D.; Bruyn, H.D.; Tahmaseb, A. Current state of the art of computer-guided implant surgery. *Periodontology 2000* **2017**, *73*, 121–133. [[CrossRef](#)]
17. Morton, D.; Phasuk, K.; Polido, W.D.; Lin, W.-S. Consideration for Contemporary Implant Surgery. *Dent. Clin. N. Am.* **2019**, *63*, 309–329. [[CrossRef](#)]
18. Mora, M.A.; Chenin, D.L.; Arce, R.M. Software Tools and Surgical Guides in Dental-Implant-Guided Surgery. *Dent. Clin. N. Am.* **2014**, *58*, 597–626. [[CrossRef](#)]
19. Minervini, G.; Romano, A.; Petrucci, M.; Maio, C.; Serpico, R.; Di Stasio, D.; Lucchese, A. Oral-facial-digital syndrome (OFD): 31-year follow-up management and monitoring. *J. Biol. Regul. Homeost. Agents* **2018**, *32*, 127–130.
20. Minervini, G.; Romano, A.; Petrucci, M.; Maio, C.; Serpico, R.; Lucchese, A.; Candotto, V.; Di Stasio, D. Telescopic overdenture on natural teeth: Prosthetic rehabilitation on (OFD) syndromic patient and a review on available literature. *J. Biol. Regul. Homeost. Agents* **2018**, *32*, 131–134.
21. Mossey, P.A.; Little, J.; Munger, R.G.; Dixon, M.J.; Shaw, W.C. Cleft lip and palate. *Lancet Lond. Engl.* **2009**, *374*, 1773–1785. [[CrossRef](#)]
22. d’Apuzzo, F.; Minervini, G.; Grassia, V.; Rotolo, R.P.; Perillo, L.; Nucci, L. Mandibular Coronoid Process Hypertrophy: Diagnosis and 20-Year Follow-Up with CBCT, MRI and EMG Evaluations. *Appl. Sci.* **2021**, *11*, 4504. [[CrossRef](#)]
23. Antonelli, A.; Bennardo, F.; Brancaccio, Y.; Barone, S.; Femiano, F.; Nucci, L.; Minervini, G.; Fortunato, L.; Attanasio, F.; Giudice, A. Can Bone Compaction Improve Primary Implant Stability? An In Vitro Comparative Study with Osseodensification Technique. *Appl. Sci.* **2020**, *10*, 8623. [[CrossRef](#)]
24. Flügge, T.; Kernen, F.; Nelson, K. Die digitale Prozesskette in der Implantologie. *Zahnmed. Up2date* **2019**, *13*, 507–530. [[CrossRef](#)]
25. Yuzbasioglu, E.; Kurt, H.; Turunc, R.; Bilir, H. Comparison of digital and conventional impression techniques: Evaluation of patients’ perception, treatment comfort, effectiveness and clinical outcomes. *BMC Oral Health* **2014**, *14*, 10. [[CrossRef](#)]
26. Warrer, K.; Buser, D.; Lang, N.P.; Karring, T. Plaque-induced peri-implantitis in the presence or absence of keratinized mucosa. An experimental study in monkeys. *Clin. Oral Implant. Res.* **1995**, *6*, 131–138. [[CrossRef](#)]
27. Chung, D.M.; Oh, T.-J.; Shotwell, J.L.; Misch, C.E.; Wang, H.-L. Significance of keratinized mucosa in maintenance of dental implants with different surfaces. *J. Periodontol.* **2006**, *77*, 1410–1420. [[CrossRef](#)]
28. Chiu, Y.-W.; Lee, S.-Y.; Lin, Y.-C.; Lai, Y.-L. Significance of the width of keratinized mucosa on peri-implant health. *J. Chin. Med. Assoc. J. CMA* **2015**, *78*, 389–394. [[CrossRef](#)]
29. Chackartchi, T.; Romanos, G.E.; Sculean, A. Soft tissue-related complications and management around dental implants. *Periodontology 2000* **2019**, *81*, 124–138. [[CrossRef](#)]
30. Bouri, A.; Bissada, N.; Al-Zahrani, M.S.; Faddoul, F.; Nouneh, I. Width of keratinized gingiva and the health status of the supporting tissues around dental implants. *Int. J. Oral Maxillofac. Implant.* **2008**, *23*, 323–326.
31. Schrott, A.R.; Jimenez, M.; Hwang, J.-W.; Fiorellini, J.; Weber, H.-P. Five-year evaluation of the influence of keratinized mucosa on peri-implant soft-tissue health and stability around implants supporting full-arch mandibular fixed prostheses. *Clin. Oral Implant. Res.* **2009**, *20*, 1170–1177. [[CrossRef](#)]
32. Mehta, P.; Lim, L.P. The width of the attached gingiva—much ado about nothing? *J. Dent.* **2010**, *38*, 517–525. [[CrossRef](#)] [[PubMed](#)]
33. Rocuzzo, M.; Grasso, G.; Dalmasso, P. Keratinized mucosa around implants in partially edentulous posterior mandible: 10-year results of a prospective comparative study. *Clin. Oral Implant. Res.* **2016**, *27*, 491–496. [[CrossRef](#)]
34. Strub, J. *Curriculum Prothetik Band 1*; 4., überarbeitete Auflage; Quintessenz: Berlin, Germany; Barcelona, Spain; Beijing, China; Chicago, IL, USA; Istanbul, Turkey; Copenhagen, Denmark; London, UK; Mailand, Italy; Moskau, Russia; Neu-Delhi, India; Paris, France; Prag, Czech Republic; São Paulo, Brazil; Seoul, Korea; Tokio, Japan; und Warschau, Poland, 2010; ISBN 978-3-86867-026-4.
35. Kihara, H.; Hatakeyama, W.; Komine, F.; Takafuji, K.; Takahashi, T.; Yokota, J.; Oriso, K.; Kondo, H. Accuracy and practicality of intraoral scanner in dentistry: A literature review. *J. Prosthodont. Res.* **2020**, *64*, 109–113. [[CrossRef](#)] [[PubMed](#)]
36. Sawase, T.; Kuroshima, S. The current clinical relevancy of intraoral scanners in implant dentistry. *Dent. Mater. J.* **2020**, *39*, 57–61. [[CrossRef](#)]
37. Tarnow, D.P.; Pérez, J.M.; Ghamid, S.S.; Manasse, M.; Froum, S.J.; Shabeesh, M.; Cho, S.-C. A New Technique to Identify the Location of the Mucogingival Junction on Computer Tomographic Scans Before Implant Placement. *Implant Dent.* **2015**, *24*, 338–342. [[CrossRef](#)]
38. Kaku, T.; Ogino, Y.; Matsushita, Y.; Koyano, K. Technique for identifying keratinized gingival tissue and soft tissue morphology on 3-dimensional implant-planning software images. *J. Prosthodont. Res.* **2016**, *116*, 21–24. [[CrossRef](#)]
39. Kuralt, M.; Gašperšič, R.; Fidler, A. 3D computer-aided treatment planning in periodontology: A novel approach for evaluation and visualization of soft tissue thickness. *J. Esthet. Restor. Dent.* **2020**, *32*, 457–462. [[CrossRef](#)] [[PubMed](#)]
40. Schlager, S. Morpho and Rvcg—Shape Analysis in R: R-Packages for Geometric Morphometrics, Shape Analysis and Surface Manipulations. In *Statistical Shape and Deformation Analysis*; Zheng, G., Li, S., Székely, G., Eds.; Academic Press: Cambridge, MA, USA, 2017; pp. 217–256, ISBN 978-0-12-810493-4.

41. Schlager, S. 3D data analysis using R. In *3D Data Acquisition for Bioarchaeology, Forensic Anthropology, and Archaeology*; Elsevier: Amsterdam, The Netherlands, 2019; pp. 131–159.
42. Schlager, S.; Statismo, T. *RvtkStatismo: Integrating Statismo and R Using the vtkStandardMeshRepresenter*; GitHub repository, 2015.
43. R Foundation for Statistical Computing. *R: A Language and Environment for Statistical Computing*; R Core Team: Vienna, Austria, 2020.
44. Fedorov, A.; Beichel, R.; Kalpathy-Cramer, J.; Finet, J.; Fillion-Robin, J.-C.; Pujol, S.; Bauer, C.; Jennings, D.; Fennessy, F.; Sonka, M.; et al. 3D Slicer as an Image Computing Platform for the Quantitative Imaging Network. *Magn. Reson. Imaging* **2012**, *30*, 1323–1341. [[CrossRef](#)] [[PubMed](#)]
45. Gunz, P.; Mitteroecker, P.; Bookstein, F.L. Semilandmarks in Three Dimensions. In *Modern Morphometrics in Physical Anthropology*; Slice, D.E., Ed.; Developments in Primatology: Progress and Prospects; Springer: Boston, MA, USA, 2005; pp. 73–98, ISBN 978-0-387-27614-4.
46. Cootes, T.F.; Taylor, C.J. *Statistical Models of Appearance for Computer Vision*; Imaging Science and Biomedical Engineering, University of Manchester: Manchester, UK, 2004; pp. 12–28.
47. Cootes, T.; Hill, A.; Taylor, C.; Haslam, J. Use of active shape models for locating structures in medical images. *Image Vis. Comput.* **1994**, *12*, 355–365. [[CrossRef](#)]
48. Fuessinger, M.A.; Schwarz, S.; Neubauer, J.; Cornelius, C.-P.; Gass, M.; Poxleitner, P.; Zimmerer, R.; Metzger, M.C.; Schlager, S. Virtual reconstruction of bilateral midfacial defects by using statistical shape modeling. *J. Cranio-Maxillofac. Surg. Off. Publ. Eur. Assoc. Cranio-Maxillofac. Surg.* **2019**, *47*, 1054–1059. [[CrossRef](#)]
49. Fuessinger, M.A.; Schwarz, S.; Cornelius, C.P.; Metzger, M.C.; Ellis, E.; Probst, F.; Semper-Hogg, W.; Gass, M.; Schlager, S. Planning of skull reconstruction based on a statistical shape model combined with geometric morphometrics. *Int. J. Comput. Assist. Radiol. Surg.* **2018**, *13*, 519–529. [[CrossRef](#)] [[PubMed](#)]
50. Semper-Hogg, W.; Fuessinger, M.A.; Schwarz, S.; Ellis, E.; Cornelius, C.P.; Probst, F.; Metzger, M.C.; Schlager, S. Virtual reconstruction of midface defects using statistical shape models. *J. Craniomaxillofac. Surg.* **2017**, *45*, 461–466. [[CrossRef](#)] [[PubMed](#)]
51. Fuessinger, M.A.; Schwarz, S.; Gass, M.; Poxleitner, P.; Brandenburg, L.; Schlager, S.; Metzger, M.C. The statistical shape model as a quality assurance measure in the treatment of complex midface fractures: A case control study. *Head Face Med.* **2021**, *17*, 44. [[CrossRef](#)] [[PubMed](#)]
52. Gass, M.; Füßinger, M.A.; Metzger, M.C.; Schwarz, S.; Bähr, J.D.; Brandenburg, L.; Weingart, J.; Schlager, S. Virtual reconstruction of orbital floor defects using a statistical shape model. *J. Anat.* **2022**, *240*, 323–329. [[CrossRef](#)] [[PubMed](#)]
53. Brandenburg, L.S.; Schwarz, S.J.; Spies, B.C.; Weingart, J.V.; Georgii, J.; Jung, B.; Burkhardt, F.; Schlager, S.; Metzger, M.C. Creating an anatomical wax-up in partially edentulous patients by means of a statistical shape model. *Int. J. Comput. Dent.* **2022**. [[CrossRef](#)]
54. Lüthi, M.; Albrecht, T.; Vetter, T. Probabilistic modeling and visualization of the flexibility in morphable models. In Proceedings of the IMA International Conference on Mathematics of Surfaces, York, UK, 7–9 September 2009; Springer: Berlin/Heidelberg, Germany, 2009; pp. 251–264.
55. Lüthi, M.; Blanc, R.; Albrecht, T.; Gass, T.; Goksel, O.; Büchler, P.; Kistler, M.; Bousleiman, H.; Reyes, M.; Cattin, P.; et al. Statismo—A framework for PCA based statistical models. *Insight J.* **2012**, *2012*, 1–18. [[CrossRef](#)]
56. Albrecht, T.; Lüthi, M.; Gerig, T.; Vetter, T. Posterior shape models. *Med. Image Anal.* **2013**, *17*, 959–973. [[CrossRef](#)] [[PubMed](#)]
57. Chen, Y.-W.; Stanley, K.; Att, W. Artificial intelligence in dentistry: Current applications and future perspectives. *Quintessence Int.* **2020**, *51*, 248–257. [[CrossRef](#)] [[PubMed](#)]
58. Grischke, J.; Johannsmeier, L.; Eich, L.; Griga, L.; Haddadin, S. Dentronics: Towards robotics and artificial intelligence in dentistry. *Dent. Mater. Off. Publ. Acad. Dent. Mater.* **2020**, *36*, 765–778. [[CrossRef](#)] [[PubMed](#)]
59. Di Stasio, D.; Romano, A.; Paparella, R.S.; Gentile, C.; Serpico, R.; Minervini, G.; Candotto, V.; Laino, L. How social media meet patients' questions: YouTube (TM) review for mouth sores in children. *J. Biol. Regul. Homeost. Agents* **2018**, *32*, 117–121. [[PubMed](#)]
60. Chee, W.W.L.; Cho, G.C.; Ha, S. Replicating Soft Tissue Contours on Working Casts for Implant Restorations. *J. Prosthodont.* **1997**, *6*, 218–220. [[CrossRef](#)] [[PubMed](#)]
61. Kolte, R.; Kolte, A.; Mahajan, A. Assessment of gingival thickness with regards to age, gender and arch location. *J. Indian Soc. Periodontol.* **2014**, *18*, 478–481. [[CrossRef](#)] [[PubMed](#)]
62. Agarwal, V.; Mehrota, N.; Vijay, V. Gingival biotype assessment: Variations in gingival thickness with regard to age, gender, and arch location. *Indian J. Dent. Sci.* **2017**, *9*, 12–15. [[CrossRef](#)]
63. Chappuis, V.; Araújo, M.G.; Buser, D. Clinical relevance of dimensional bone and soft tissue alterations post-extraction in esthetic sites. *Periodontology 2000* **2017**, *73*, 73–83. [[CrossRef](#)] [[PubMed](#)]
64. Matheny, M.; Israni, S.T.; Ahmed, M.; Whicher, D. *Artificial Intelligence in Health Care: The Hope, the Hype, the Promise, the Peril*; NAM Special Publication; National Academy of Sciences: Washington, DC, USA, 2019.
65. Schwendicke, F.; Samek, W.; Krois, J. Artificial Intelligence in Dentistry: Chances and Challenges. *J. Dent. Res.* **2020**, *99*, 769–774. [[CrossRef](#)] [[PubMed](#)]
66. Müller, A.; Mertens, S.M.; Göstemeyer, G.; Krois, J.; Schwendicke, F. Barriers and Enablers for Artificial Intelligence in Dental Diagnostics: A Qualitative Study. *J. Clin. Med.* **2021**, *10*, 1612. [[CrossRef](#)] [[PubMed](#)]